Applied and Computational Mechanics 7 (2013) 137–144

# Identification of parameters of cohesive elements for modeling of adhesively bonded joints of epoxy composites

R. Kottner[a,*], R. Hynek[b], T. Kroupa[a]

[a] European Centre of Excellence, NTIS – New Technologies for Information Society, Faculty of Applied Sciences, UWB in Pilsen, Univerzitní 22, 306 14 Plzeň, Czech Republic

[b] Department of Mechanics, Faculty of Applied Sciences, UWB in Pilsen, Univerzitní 22, 306 14 Plzeň, Czech Republic

Received 25 August 2013; received in revised form 29 November 2013

**Abstract**

Adhesively bonded joints can be numerically simulated using the cohesive crack model. The critical strain energy release rate and the critical opening displacement are the parameters which must be known when cohesive elements in MSC.Marc software are used. In this work, the parameters of two industrial adhesives Hunstman Araldite 2021 and Gurit Spabond 345 for bonding of epoxy composites are identified. Double Cantilever Beam (DCB) and End Notched Flexure (ENF) test data were used for the identification. The critical opening displacements were identified using an optimization algorithm where the tests and their numerical simulations were compared.


*Keywords:* adhesively bonded composite, DCB and ENF tests, cohesive elements, identification, Araldite 2021, Spabond 345, finite element model

## 1. Introduction

Adhesively bonded joints have very high utilization in fiber reinforced composite structures. These joints are light, corrosion resistant and do not reduce the strength of jointed components. The increased application of the adhesive joints has been accompanied by the development of mathematical models to analyze the behavior of these joints [4]. The use of so-called cohesive crack model for the modeling of the joints is one of the most appealing techniques. It has been developed since 1960s [2]. The aim of this work is the identification of the parameters of the cohesive crack model for two adhesives (Hunstman Araldite 2021, Gurit Spabond 345) applied on unidirectional carbon fiber reinforced composite modeled in the MSC.Marc 2010 system [6].

## 2. Theory

MSC.Marc 2010 system has a library of so-called interface (cohesive) elements [6], which can be used to simulate adhesively bonded joints. The constitutive behavior of these elements is expressed in terms of tractions versus opening displacements between the cohesive element faces which belong to the bonded surfaces. The dependence of traction $t$ on opening displacement $v$ can be expressed using three different functions: an exponential, a bilinear, and a linear-exponential (Fig. 1). The area bellow the functions is critical strain energy release rate $G_c$. The functions are characterized by an initial reversible response followed by an irreversible response as soon as a critical opening displacement $v_c$ has been reached. Critical strain energy release rate $G_c$ and critical opening displacement $v_c$ are the parameters that has to be identified.

*Corresponding author. Tel.: +420 377 632 373, e-mail: kottner@kme.zcu.cz.

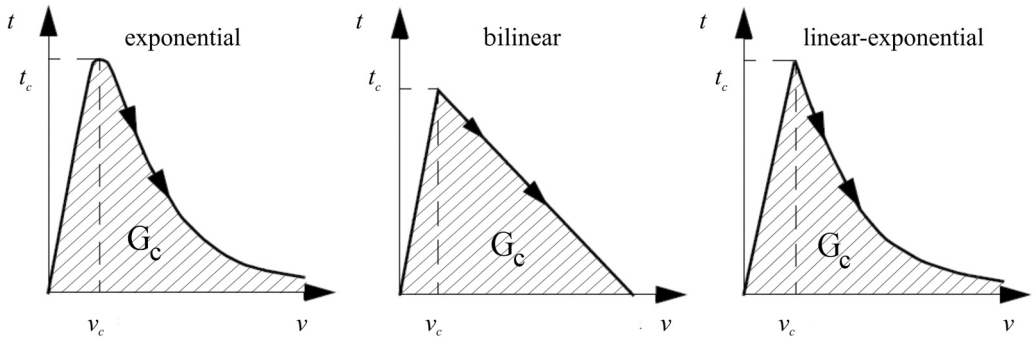


Fig. 1. Types of cohesive models

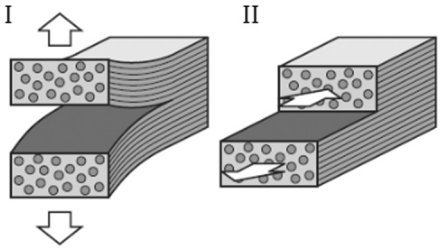


Fig. 2. Failure modes of adhesively bonded composites

Two basic modes I resp. II of the joint failure are described as failures under tensile and shear loading, respectively (Fig. 2) [3]. Every failure can be described as a superposition of these basic modes. Double Cantilever Beam (DCB) test induces failure in mode I whereas End Notched Flexure (ENF) test induces failure in mode II (see Figs. 3 and 4).

Parameters $G_{\mathrm{Ic}}$ and $G_{\mathrm{IIc}}$ can be calculated directly from experimental data using the modified beam theory method [3, 9] as

$$G_{\mathrm{Ic}} = \frac{3F_{\mathrm{c}}\delta_{\mathrm{c}}}{2b(a+\Delta)}, \tag{1}$$

$$G_{\mathrm{IIc}} = \frac{9a^2F_{\mathrm{c}}\delta_{\mathrm{c}}}{2b(2L^3+3a^3)}, \tag{2}$$

where $F_{\mathrm{c}}$ is critical value of the applied force that causes the first failure, $\delta_{\mathrm{c}}$ critical value of the load point displacement, $b$ initial crack width (sample width), $a$ initial crack length, $\Delta$ crack length correction according to ASTM D5528-01 [1], and $L$ is distance between the load point and the supports in case of the ENF test.

## 3. Experiment

Unidirectional carbon fiber reinforced composite (Tenax HTS 5631) plates were bonded using Araldite 2021 and Spabond 345 adhesives. Material parameters of the composite plates were investigated in previous work where only tensile and compression tests were performed [5]. Identified parameters are listed in Table 1 [5]. The plates were bonded according to the DCB and ENF test schemes (Figs. 3 and 4). Dimensions of the specimens are listed in Table 2. Zwick/Roell Z050 testing device was used. Specimens were loaded by speed of 5 mm/min. Examples of obtained force-displacement curves are shown in Figs. 8–11.

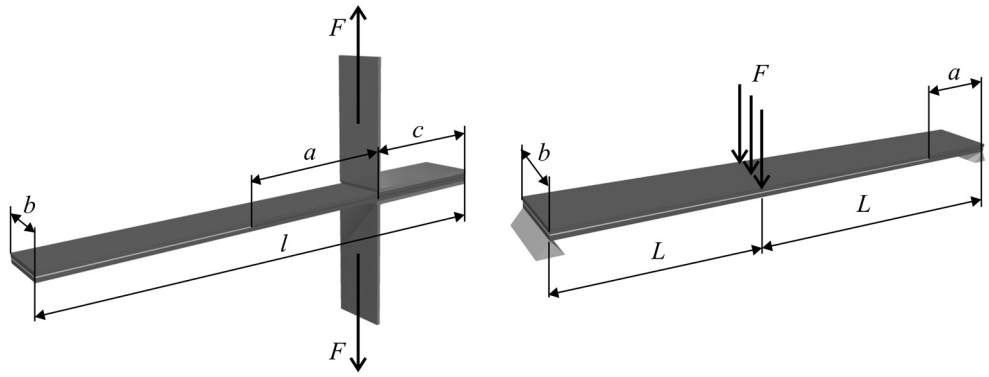


Fig. 3. Schemes of DCB (left) and ENF experiments

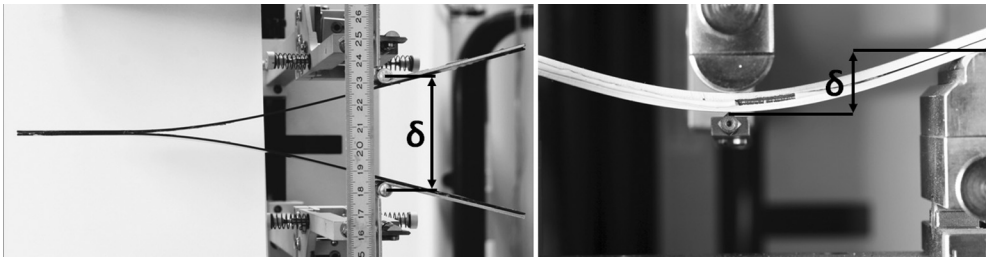


Fig. 4. DCB (left) and ENF experiments, load point displacement $\delta$

Table 1. Tenax HTS 5631 composite material parameters

| | |
|---|---|
| $E_{11}$ [GPa] | 100.00 (120.00) |
| $E_{22}$ [GPa] | 8.00 |
| $E_{33}$ [GPa] | 8.00 |
| $G_{12}$ [GPa] | 4.00 |
| $G_{23}$ [GPa] | 3.04 |
| $G_{31}$ [GPa] | 4.00 |
| $\nu_{12}$ | 0.337 |
| $\nu_{23}$ | 0.315 |
| $\nu_{31}$ | 0.022 |

Table 2. Dimensions of experimental specimens

| test type | $a$ [mm] | $b$ [mm] | $l$ [mm] | $L$ [mm] | $t$ [mm] |
|---|---|---|---|---|---|
| DCB | 80/35 | 30/20 | 250/150 | – | 5 |
| ENF | 35 | 20 | – | 60 | 5 |

## 4. Parameters identification

Parameters $G_{\mathrm{Ic}}$ and $G_{\mathrm{IIc}}$ were calculated directly from experimental data using Eqs. (1) and (2). Critical opening displacements $v_c$ related to both I and II modes could not be calculated directly using the experimental data. For each mode, this parameter was fit using a comparison of the experiments and their numerical simulations in an identification procedure described below.

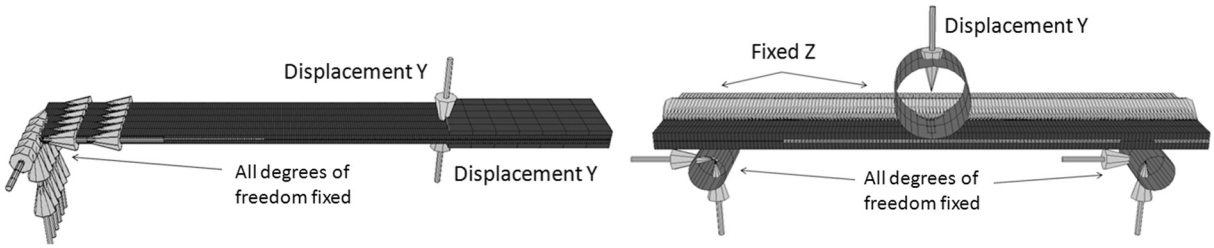


Fig. 5. Boundary conditions of FE models of DCB (left) and ENF experiments

Finite element (FE) models of the experiments were performed in the FE method system MSC.Marc 2010 (Fig. 5). Linear brick elements were used. In the case of DCB, each composite plate was loaded by half of total displacement at appropriate nodes on steel hinges. Touching contact between rigid cylindrical surfaces and deformable composite plate was considered in the ENF test simulation. Loading displacement was applied on a control node of the middle rigid surface. A symmetry was used to decrease number of elements and computing time.

Young's modulus $E_{11}$ of the composite plates in tension is 120 GPa [5]. Value of this modulus has fundamental influence on the composite plate bending stiffness because the orientation of fibers of the composite plates were parallel to the longitudinal direction. Since the Young's modulus identified using tensile and bending tests shows different values, the $E_{11}$ value was fitted using the comparison of bending test of one composite plate (without any joint) and its numerical simulation. The value changed to $E_{11} = 100$ GPa. Thereafter, cohesive parameter $v_c$ could be identified.

The experiments and the numerical simulations were compared using standard residual function that was used e.g. in [8]

$$R = \sum_{i=1}^{n} (F_{i,\,\mathrm{FEM}} - F_{i,\,\mathrm{EXP}})^2, \tag{3}$$

where $F_{\mathrm{FEM}}$ and $F_{\mathrm{EXP}}$ are the values of forces obtained from model and experiment, respectively, and $n$ is number of points where results were compared. Number $n$ corresponded to the number of time increments of a FE analysis, time increments had identical length. Function represents the sum of differences between FE analysis and experiment in these points of comparison.

The identification procedure is obvious from Fig. 6. The gradient optimization algorithm NLPQLP [7] was used for the identification of parameters using optiSLang software. The procedure control and residual calculations were performed using Matlab scripts.

## 5. Results

Although the specimens with Araldite 2021 usually failed slowly and smoothly with pure cohesive crack, the specimens with Spabond 345 cracked with large displacement jumps and the failure surface showed mix of adhesive and cohesive failures. Since the cohesive model is not capable of correct description of such behavior, the displacement interval considered in the Spabond 345 residual expression ended with $\delta_{\mathrm{d}}$ that is displacement value where the first crack propagation stopped (see Fig. 7).

Figs. 8–11 show result comparison of the experiments and the simulations. The exponential behavior (Fig. 1) of the cohesive elements was assumed in presented results. This assumption

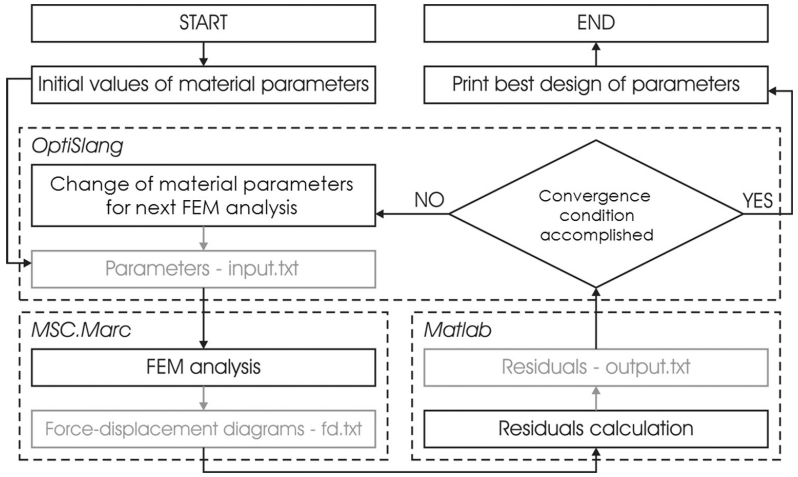


Fig. 6. Procedure of identification of critical opening displacement

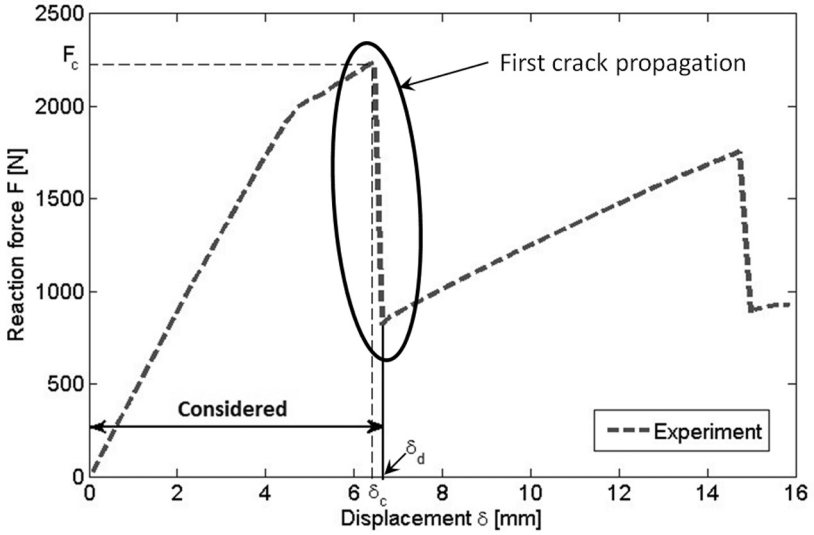


Fig. 7. Displacement interval considered in the Spabond 345 residual expression

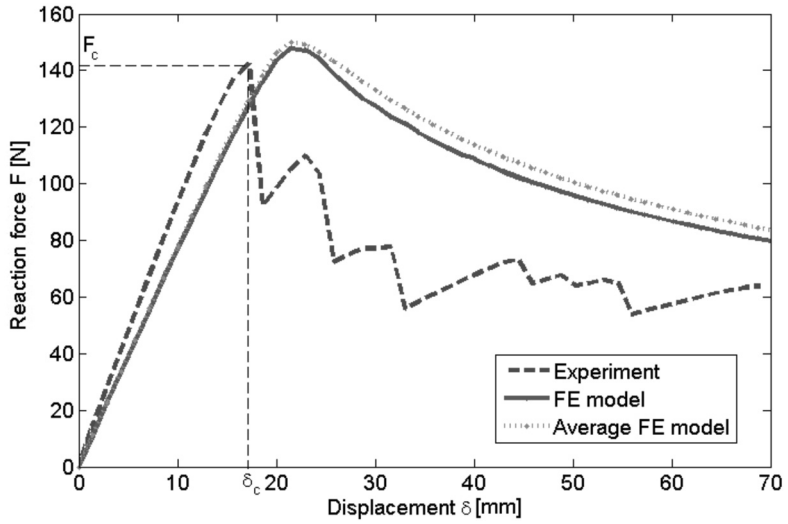


Fig. 8. Force-displacement curve of an experiment, FE model of a specimen and model with identified (averaged) parameters, Araldite 2021 adhesive, DCB test

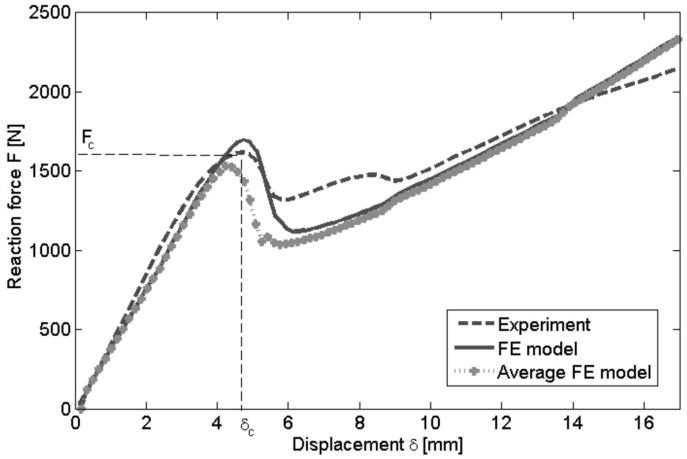


Fig. 9. Force-displacement curve of an experiment, FE model of a specimen and model with identified (averaged) parameters, Araldite 2021 adhesive, ENF test

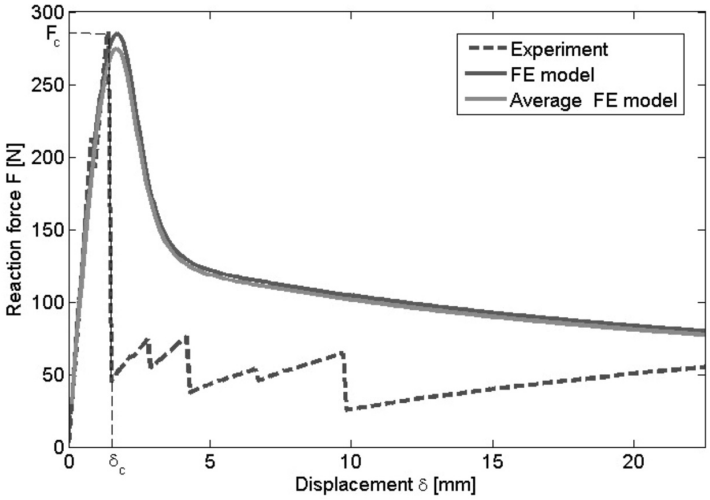


Fig. 10. Force-displacement curve of an experiment, FE model of a specimen and model with identified (averaged) parameters, Spabond 345 adhesive, DCB test

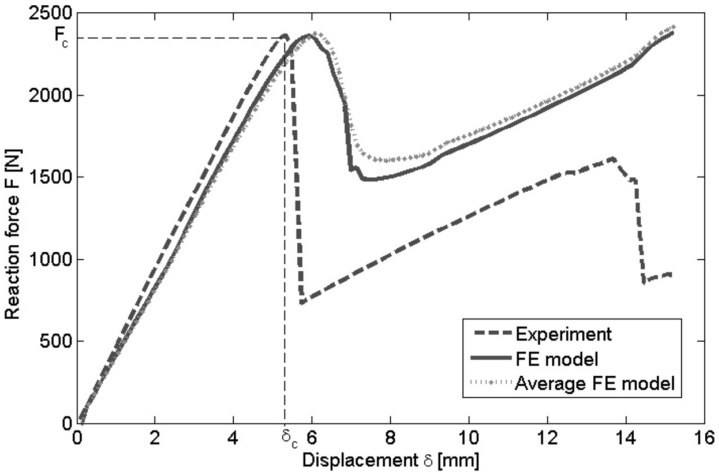


Fig. 11. Force-displacement curve of an experiment, FE model of a specimen and model with identified (averaged) parameters, Spabond 345 adhesive, ENF test

allowed achievement of lowest residuals according to Eq. (3). Because of differences in experimental specimens (size of bonded surfaces, composite plate thickness) each specimen test was simulated separately. After all specimen simulations according to test and adhesive types, averaged values of identified parameters were calculated. In the result comparisons, experimental curves of selected specimens and their simulations are shown together with curves from simulations where average values of the identified parameters were used.

Values of the identified parameters (the averaged values) are listed in Table 3. It is obvious that simulations exhibit higher values of the reaction forces after critical value $F_c$ than the experiments. Unfortunately, considering equal values of the critical strain energy release rate in every cohesive element, better agreement could not be achieved.

Table 3. Identified parameters

| | Hunstman Araldite 2021 | Gurit Spabond 345 |
|---|---|---|
| $G_{\mathrm{Ic}}$ [J/m$^2$] | 1 604 | 1 325 |
| $G_{\mathrm{IIc}}$ [J/m$^2$] | 3 174 | 7 027 |
| $v_{\mathrm{Ic}}$ [$\mu$m] | 38.3 | 113.0 |
| $v_{\mathrm{IIc}}$ [$\mu$m] | 49.2 | 68.4 |

## 6. Conclusion

Parameters of two adhesives (Hunstman Araldite 2021, Gurit Spabond 345), which are necessary for modeling of bonded joints using the cohesive crack model, were identified. The knowledge of the joint behavior until the first joint failure (the first failure corresponds to the critical value of reaction force $F_c$) is the most important. To describe the joint behavior after the first failure more precisely, the critical strain energy release rate should have different values in the cohesive elements that represent the initial location of the crack and in the rest of cohesive elements. The measurement of these values is performed by precracked samples but, in this case, precise determination of the crack length is complicated. Moreover, if the type of the crack is not purely cohesive (Spabond 345 in this work), the disagreement after the first joint failure increases.

## Acknowledgements

This work was supported by the European Regional Development Fund (ERDF), project "NTIS – New Technologies for Information Society", European Centre of Excellence, CZ.1.05/1.1.00/02.0090 and by the projects GA P101/11/0288.

## References

[1] ASTM D5528-01, Standard test method for mode I interlaminar fracture toughness of unidirectional fiber-reinforced polymer matrix composites, ASTM International, 2002.

[2] Borg, R., Nilsson, L., Simonsson, K., Simulating DCB, ENF and MMB experiments using shell elements and a cohesive zone model, Composites Science and Technology 64 (2) (2004) 269–278.

[3] Ducept, F., Davies, P., Gamby, D., Mixed mode failure criteria for a glass/epoxy composite and an adhesively bonded composite/composite joint, International Journal of Adhesion and Adhesives 20 (3) (2000) 233–244.

[4] Goncalves, J. P. M., de Moura, M. F. S. F., de Castro, P. M. S. T., A three-dimensional finite element model for stress analysis of adhesive joints, International Journal of Adhesion and Adhesives 22 (5) (2002) 357–365.

[5] Krystek, J., Kroupa, T., Kottner, R., Identification of mechanical properties from tensile and compression tests of unidirectional carbon composite, Proceedings of the $48^{\text{th}}$ International Scientific Conference on Experimental Stress Analysis 2010, Velke Losiny, Palacky University, 2010, pp. 193–200.

[6] MSC.Software, Marc 2010 volume A: Theory and user information, MSC.Software Corporation, 2010.

[7] optiSLang, Sensitivity analysis, multidisciplinary optimization, robustness evaluation, reliability analysis and robust design optimization, optiSLang Documentation, Version 3.2.1, DYNARDO GmbH, 2011.

[8] Zemčík, R., Kottner, R.,Laš, V., Plundrich, T., Identification of material properties of quasi-unidirectional carbon-epoxy composite using modal analysis, Materiali in Tehnologije 43 (5) (2009) 257–260.

[9] Zemčík, R., Laš, V., Numerical and experimental analyses of the delamination of cross-ply laminates, Materiali in Tehnologije 42(4) (2008) 171–174.